

## PREDICTION OF FORMING LIMIT IN STRETCH FLANGING BY FINITE ELEMENT SIMULATION COMBINED WITH DUCTILE FRACTURE CRITERION

HIROHIKO TAKUDA<sup>1</sup>, TAKAYUKI HAMA<sup>1</sup>, KAZUKI NISHIDA<sup>1</sup>, TOHRU YOSHIDA<sup>2</sup>, JUN NITTA<sup>2</sup>

<sup>1</sup>Department of Energy Science and Technology, Kyoto University, 606-8501 Kyoto, Japan

<sup>2</sup>Steel Research Laboratories, Nippon Steel Corporation, 293-8511 Futtsu, Japan

Corresponding author: [takuda@energy.kyoto-u.ac.jp](mailto:takuda@energy.kyoto-u.ac.jp) (H. Takuda)

### Abstract

In our previous studies, the limit strains of a few types of high-strength steel sheets under various strain paths from balanced biaxial to uniaxial tension were measured and compared with those derived from some criteria for ductile fracture. It turned out that the fracture strains derived from the criterion by Cockcroft and Latham gave the best fit to the experimental results. In this study, the criterion is applied to the prediction of forming limit in stretch flanging. The stretch flanging tests of a high-strength steel sheet are simulated by the dynamic explicit finite element program LS-DYNA ver. 971 with shell elements. The comparison of the simulated results with the experimental results shows that the forming limit in stretch flanging is successfully predictable by the present approach when the work hardening and damage of the sheet edge in the blanking process are taken into consideration.

**Key words:** Sheet metal forming, FEM, stretch flanging, ductile fracture criterion

## 1. INTRODUCTION

The authors have recently proposed an approach to predict the forming limit in sheet forming processes by introducing criteria for ductile fracture into the finite element simulation [1-4]. In the criteria the occurrence of ductile fracture is estimated by the macroscopic stress and strain during forming which are calculated by the finite element simulation. In our previous studies [5,6], the possibility of the application of some criteria for ductile fracture to high-strength steel sheets was examined. Due to the less formability the forming limit prediction is very important to find the forming conditions suitable for high-strength steel sheets. The forming limits of a few types of high-strength steel sheets under various strain paths from balanced biaxial to uniaxial tension were examined by the Marciniak-type in-plane biax-

ial stretching test [7], and they were compared with those derived from the ductile fracture criteria. As a result, it was found that the fracture strains derived from the criterion by Cockcroft and Latham [8] gave the best fit to the experimental results. Then, the forming limit predictions were successfully carried out for 3-dimensional deep drawing and stretching processes by the finite element simulation combined with the ductile fracture criterion.

Stretch flanging is also one of the fundamental press forming processes like deep drawing and stretching, but is different from others in the point that fracture occurs at the edge of the sheet. The sheet edge suffers influences of the pre-forming, i.e. blanking. In this study, stretch flanging tests of a 780 MPa grade high-strength steel sheet are carried out for various blank geometries, and they are simulated by the dynamic explicit finite element program LS-

DYNA ver.971 combined with the ductile fracture criterion. The forming limits are predicted by taking the influences of the blanking process into consideration.

2. EXPERIMENTAL PROCEDURE

2.1. Material

In this study, a zinc-coated high-strength steel sheet of 780 MPa grade with a thickness of 1.4 mm is used. Table 1 shows the tensile properties of the sheet with average values in the 0, 45 and 90° directions to rolling except for *r*-value. *K*- and *n*-values in the table correspond to the coefficients in the following approximation of flow stress.

$$\bar{\sigma} = K\bar{\varepsilon}^n \tag{1}$$

The ductile fracture criterion proposed by Cockcroft and Latham is given as

$$\int_0^{\bar{\varepsilon}_f} \sigma_{\max} d\bar{\varepsilon} = C_1 \tag{2}$$

where  $\bar{\varepsilon}_f$  is the equivalent strain at which the fracture occurs,  $\sigma_{\max}$  is the maximum normal stress,  $\bar{\varepsilon}$  is the equivalent strain, and  $C_1$  is the material constant.

Table 1. Tensile properties of the sheet

<i>K</i> -value[MPa]	<i>n</i> -value	EL[%]	TS[MPa]	<i>r</i> <sub>0</sub>	<i>r</i> <sub>45</sub>	<i>r</i> <sub>90</sub>
1360	0.16	19.0	836	0.74	1.12	0.91

EL : Elongation TS : Tensile strength *r* : Normal anisotropy parameter

The fracture strains of the sheet measured by the Marciniak-type biaxial stretching tests are indicated in figure 1. Since the relationships between the fracture strains for various strain ratios and the fracture criterion were clarified in the previous studies [5,6], the fracture strains only near the plane strain condition ( $\beta = \varepsilon_2/\varepsilon_1 = 0$ ) were measured in this study in order to evaluate the material constant  $C_1$  in the criterion. The direction of major strain in the biaxial stretching tests was set to be the rolling direction. The material constant  $C_1$  was evaluated to be 710 MPa. Please refer to the reference [5] for details of calculation of fracture strain.

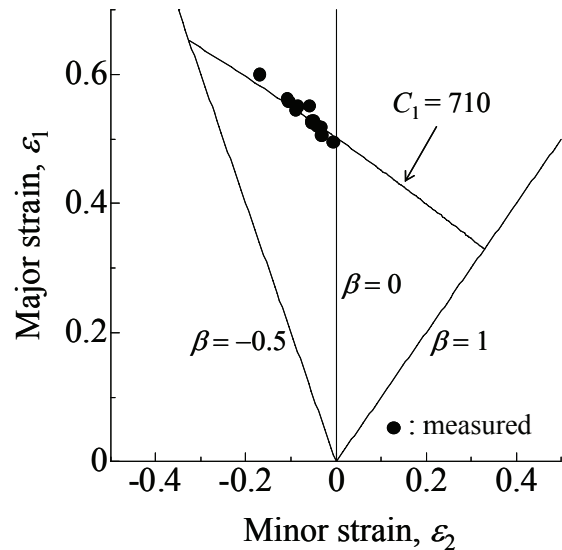


Fig. 1. Fracture strains measured by the Marciniak-type biaxial stretching tests

2.2. Stretch flanging test

From the above sheet the specimens for stretch flanging test were made. Two types of specimens with a machined edge and a blanked one, namely made by machining and blanking, were prepared. The geometries of the specimens are indicated in figure 2. The tools and specimen used for the stretch flanging tests are schematically indicated in figure 3. The specimen was set so that the *x*-direction in figure 3 corresponded to the rolling direction. The tests were carried out for various heights of flange, *H* from 10 to 35 mm and for two radii of curvature, *R* of 30 and 60 mm. The burr in case of blanked edge was set at the die side.

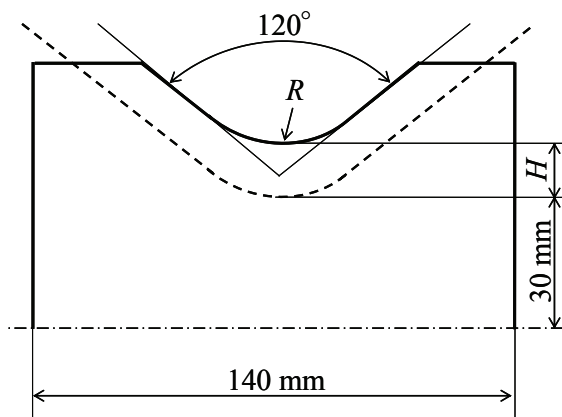


Fig. 2. Geometries of specimens (1/2 model)



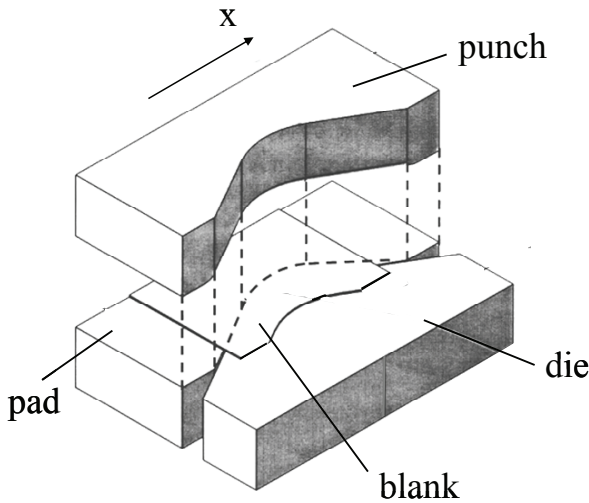


Fig. 3. Tools and specimen (1/2 model)

### 3. FINITE ELEMENT SIMULATION

In order to analyze the abovementioned stretch flanging tests, the dynamic explicit finite element program LS-DYNA ver. 971 was used in this study. For the constitutive equations, Hill's yield criterion for anisotropic material [9] and the formula for flow stress (1) were used. Coulomb's law of friction was assumed between the specimen and tools, and the frictional coefficient of 0.15 was given.

The sheet specimens were modeled in shell elements with three integration points in the thickness direction, and the element size was determined as follows. In stretch flanging fracture occurs at the edge and the gradient of strain is steep near the edge. The elements near the edge need to be divided as small as possible. In case of shell elements, however, elements smaller than the sheet thickness may cause calculation errors, as written in the user's manual of LS-DYNA. Therefore, the element meshes shown in figure 4 were adopted, where the size of elements at the edge was almost the same as the sheet thickness of 1.4 mm. As shown in this figure, the calculations were carried out for the half sections due to symmetry.

The reliability of the results calculated with the element meshes were ascertained by the strain distributions near the edge. As an example, figure 5 illustrates the measured and calculated distributions of strains at  $x = 0$  (figure 4) after a stretch flanging test for a radius  $R$  of 60 mm and a flange height  $H$  of 25 mm. The horizontal axis indicates the distance from the edge. The calculated results agree well with the measured ones.

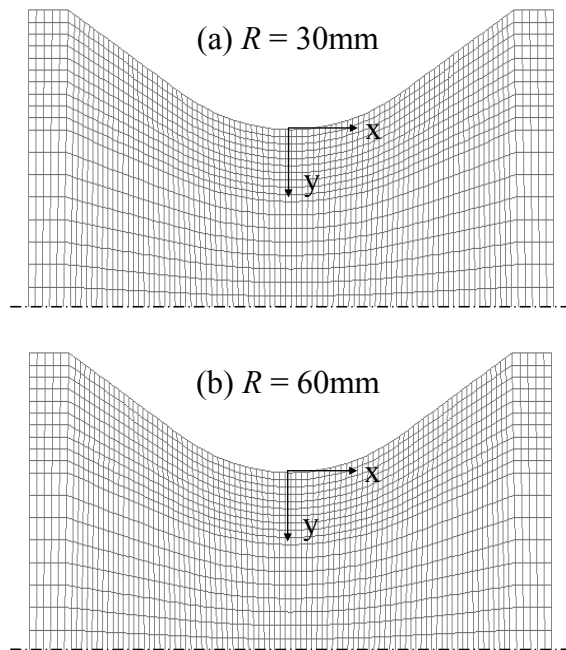


Fig. 4. Finite element meshes adopted (1/2 model)

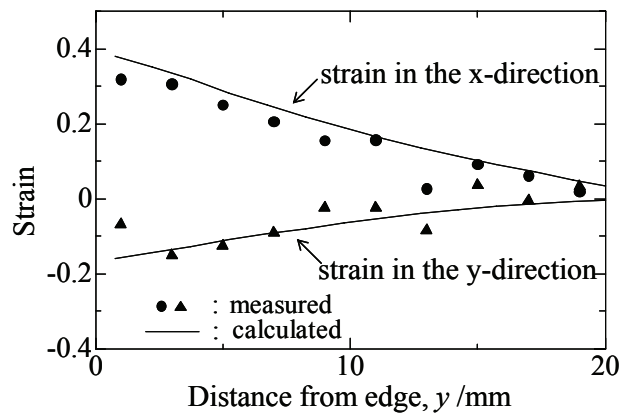


Fig. 5. Strain distributions at  $x = 0$  for  $H = 25$  mm and  $R = 60$  mm

The ductile fracture criterion (2) proposed by Cockcroft and Latham is modified and the integral  $I$  defined as

$$I = \frac{1}{C_1} \int_0^{\bar{\epsilon}} \sigma_{\max} d\bar{\epsilon} \quad (3)$$

Using the distributions of stress and strain obtained by the finite element simulation, the integral  $I$  is calculated for each integration point. The condition of fracture is satisfied when and where the integral  $I$  amounts to unity. The integral  $I$  at the integration points on the mid-surface of the sheet is used in the following results.



4. RESULTS AND DISCUSSION

4.1. Stretch flanging in case of machined edge

Figure 6 shows the specimen after stretch flanging test for  $H$  of 30 mm and  $R$  of 25 mm in case of machined edge. The fracture occurs at the center of edge. Figure 7 shows the calculated distribution of the integral  $I$  for this case. The integral  $I$  at the center of the edge amounts to unity at the punch stroke of 23.4 mm, and the fracture initiation at that site is predicted.

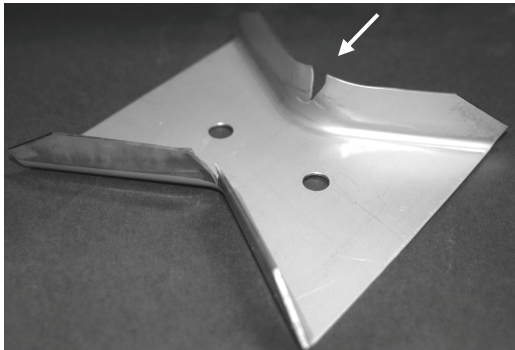


Fig. 6. Fracture at stretch flanging test for  $R = 30$  mm and  $H = 25$  mm

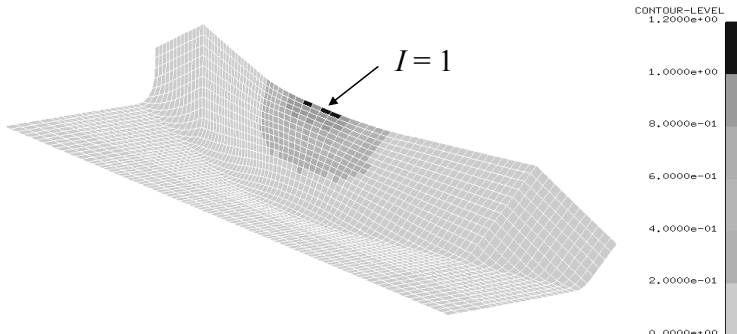


Fig. 7. Calculated distribution of integral  $I$  for  $R = 30$  mm and  $H = 25$  mm at punch stroke of 23.4 mm

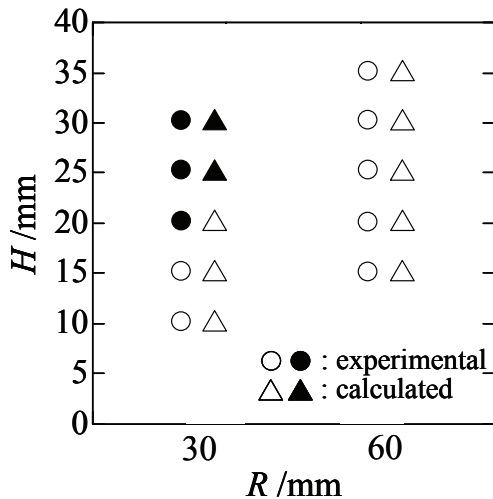


Fig. 8. Results of stretch flanging tests for machined edge

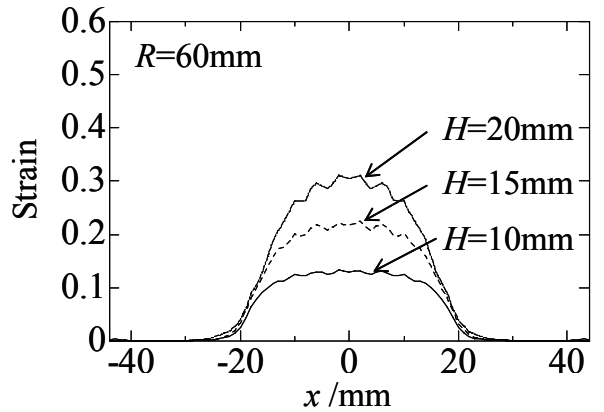
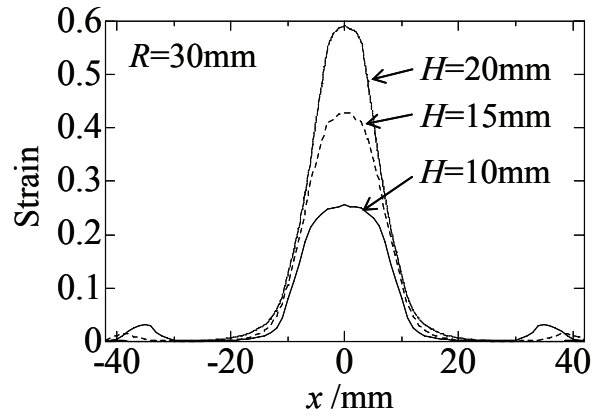


Fig. 9. Calculated distributions of strain in the  $x$ -direction at edge

The results for various  $R$  and  $H$  are indicated in figure 8. The circles and triangles indicate the experimental and calculated results, respectively. The solid marks indicate the cases where the fracture occurs during stretch flanging, and the open marks the fracture does not occur.

As shown in the calculated distributions of strain in the  $x$ -direction of figure 9, the strain at the center of edge increases with  $H$  and with decreasing  $R$ . The fracture, therefore, tends to occur with increasing  $H$  and decreasing  $R$ . The calculated results by assuming that fracture occurs when and where the integral  $I$  amounts to unity correspond well to the experimental results. It is found that the present approach is applicable to the prediction of forming limit in stretch flanging in case of machined edge.

4.2. Stretch flanging in case of blanked edge

In practice, however, the sheet is cut usually by blanking and suffers the influences of blanking. The forming limits in the present stretch flanging tests are notably lower for the blanked edge than the machined one. Without considering the influences of



blanking the forming limit cannot be correctly predicted.

From the measurement of Vickers hardness near the edge, we have known that there is no influence of pre-forming in case of machining, and that the work hardening occurs only near the edge in case of blanking. In this study, the rough approximation is adopted where the influence of blanking is given on the average as the input data to only one layer of elements at the edge (figure 4).

By substituting the pre-strain,  $\bar{\varepsilon}_0$  the work hardening is taken into consideration, and the increase in the stress brings the slight increase of the integral  $I$ . However, so predicted forming limits are still higher than the experimental ones. Next, not only the work hardening but also the damage at the blanking process is taken into consideration. Assuming the simple shear stress condition in the blanking process for convenience' sake, the integral  $I_0$  during the blanking process is given from Hill's yield criterion and equation (3) as

$$I_0 = \frac{1}{3} \sqrt{\frac{2(r+2)}{r+1}} \frac{K}{C_1(n+1)} \bar{\varepsilon}_0^{n+1} \quad (4)$$

Here, the average of  $r_0$ ,  $r_{45}$  and  $r_{90}$  is used for  $r$ -value.

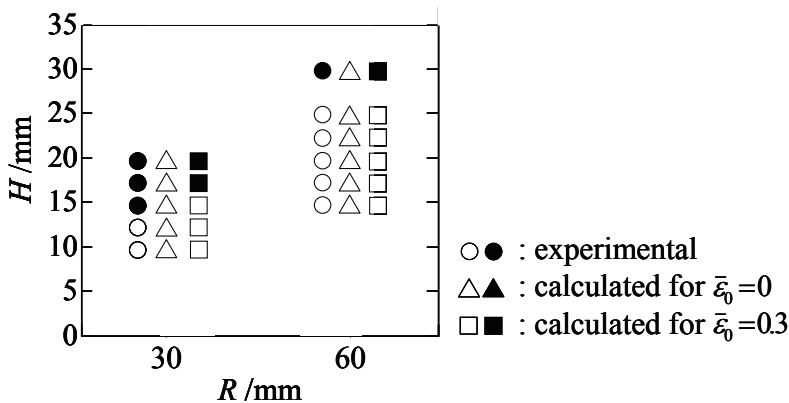


Fig. 10. Results of stretch flanging tests for blanked edge

Figure 10 shows the results of stretch flanging tests in case of blanked edge. The circles indicate the experimental results, and the solid and open marks have the same meanings as figure 8. The triangle marks indicate the predicted results without considering the influence of blanking. On the contrary, the square marks indicate the results predicted by assuming that fracture occurs when and where the total of  $I_0$  and  $I$  amounts to unity, for the pre-strain of 0.3. The predicted forming limits with considering the influence of blanking agree well with the experimental ones.

## 5. CONCLUSIONS

In this study, the ductile fracture criterion proposed by Cockcroft and Latham was combined with the finite element simulation software LS-DYNA ver. 971 and applied to the prediction of forming limit in stretch flanging of a high-strength steel sheet. It turned out that not only for the machined edge but also for the blanked edge the prediction became possible by taking the work hardening and the damage caused by the pre-strain into consideration.

Although the estimation of the pre-strain depending on the conditions of the blanking process remains to be solved in future, the possibility of prediction of the forming limit in stretch flanging by the present approach was demonstrated.

## REFERENCES

1. Takuda, H., Mori, K., Fujimoto, H., Hatta, N., 1996, Prediction of Forming Limit in Deep Drawing of Fe/Al Laminated Composite Sheets Using Ductile Fracture Criterion, *J. Mater. Process. Tech.*, 60, 291-296.
2. Takuda, H., Mori, K., Fujimoto, H., Hatta, N., 1999a, Prediction of Forming Limit in Bore-Expanding of Sheet Metals Using Ductile Fracture Criterion, *J. Mater. Process. Tech.*, 92-93, 433-438.
3. Takuda, H., Mori, K., Hatta, N., 1999b, The Application of Some Criteria for Ductile Fracture to the Prediction of the Forming Limit of Sheet Metals, *J. Mater. Process. Tech.*, 95, 116-121.
4. Takuda, H., Mori, K., Takakura, N., Yamaguchi, K., 2000, Finite Element Analysis of Limit Strains in Biaxial Stretching of Sheet Metals Allowing for Ductile Fracture, *Int. J. Mech. Sci.*, 42, 785-798.
5. Takuda, H., Kanie, T., Isogai, E., Yoshida, T., 2004, Application of Ductile Fracture Criteria to Prediction of Forming Limit of High-Strength Steel Sheets, *Steel Grips*, 2, 439-443.
6. Takuda, H., Hama, T., Yoshida, T., Nitta, J., 2008, Forming Limit Prediction of High-Strength Steel Sheets in Stretch Forming, *Steel Res. Intern.*, 79, Metal Forming 2008, 1, 19-23.
7. Marciniak, Z., Kuczynski, K., 1967, Limit Strain in the Processes of Stretch-Forming Sheet Metal, *Int. J. Mech. Sci.*, 9, 609-620.
8. Cockcroft, M.G., Latham, D.J., 1968, Ductility and the Workability of Metals, *J. Inst. Metals*, 96, 33-39.
9. Hill, R., 1950, *The Mathematical Theory of Plasticity*, Oxford University Press, Oxford, 318-321.



**OKREŚLANIE WARTOŚCI ODKSZTAŁCEŃ  
KRYTYCZNYCH W TEŚCIE TŁOCZNOŚCI  
Z WYKORZYSTANIEM SYMULACJI METODĄ  
ELEMENTÓW SKOŃCZONYCH SPRZĘŻONĄ  
Z KRYTERIUM PLASTYCZNEGO PĘKANIA**

Streszczenie

Prowadzone wcześniej przez autorów badania miały na celu określenie odkształceń granicznych w kilku typach stali o podwyższonej granicy plastyczności podczas różnych schematów obciążenia, np. dla stanu dwuosiowego lub stanu jednoosiowego. Wyniki tych badań porównano z rezultatami uzyskanymi w drodze analizy teoretycznej bazującej na kryteriach plastycznego pęknięcia. Porównanie to wykazało, iż graniczne wartości odkształcenia określone w oparciu o kryterium Cockcrofta i Lathama są najbliższe wynikom badań laboratoryjnych. W niniejszej pracy analogiczną analizę zastosowano do symulacji próby tłoczności. Przeprowadzona analiza numeryczna wykorzystuje pakiet komercyjny metody elementów skończonych LS-DYNA w wersji 971. W pracy wykorzystano elementy skończone typu powłokowego. Wyniki symulacji wykazały dużą zgodność uzyskanych wartości odkształcalności granicznej z wynikami badań laboratoryjnych. Taka zgodność była możliwa poprzez uwzględnienie w modelu numerycznym procesu umocnienia oraz pęknięcia występującego na brzegu wsadu.

---

*Submitted: September 9, 2008*

*Submitted in a revised form: October 20, 2008*

*Accepted: October 20, 2008*

